

Discrete global symmetries and dynamics of emergent fermions

Fan Yang¹ and Fei Zhou²

¹*Institute for Advanced Study, Tsinghua University, Beijing, China 100084*

²*Department of Physics and Astronomy, University of British Columbia, Vancouver, BC, Canada, V6T 1Z1*

(Dated: September 2, 2022)

Global symmetries that define the number of low energy degrees of freedom have profound consequences on universal properties near topological quantum critical points and in other gapless or nearly gapless states of emergent fermions. We take a Z_2 global symmetry (such as the time-reversal one) as an example to study its effect on thermodynamic and transport properties. Although the density of thermal entropy of Z_2 symmetric systems is simply twice of their counterparts without any global symmetries or Z_1 case, the temperature dependence of thermal conductivity κ is distinctly and drastically different for different symmetries. In the Z_2 symmetric case, we have $\kappa \propto T^{-(d-1)}$ in the quantum critical regime near weakly interacting fixed points, while for systems with no global symmetries or Z_1 case, $\kappa \propto T^{-(d+3)}$ with d the spatial dimension. Only near strong coupling fixed points, both cases with or without Z_2 global symmetries follow the single scaling function, $\kappa \propto T^{d-1}$. These distinct scalings of thermal conductivity can also appear in other gapless fermion systems, such as surface states and Majorana wires at superconductor–topological-insulator–superconductor junctions that are experimentally accessible.

Tremendous efforts have been made to understand emergent Majorana fermions in electronic systems [1–3]. Many previous studies on Majorana fermions in condensed matter have mainly focused on Majorana zero modes localized in vortices or on the edge of topological superconductors [4–14]. One major motivation of those efforts was to trap and manipulate these decoherence free states as a fundamental building block for topological quantum computers [15, 16]. On the other hand, propagating Majorana fermions as low energy emergent particles have received relatively less attention, partly because they are hard to separate experimentally. The main purpose of this Letter is to reveal some surprising collective dynamics of Majorana fermions that are distinct from complex fermions and can be potentially studied in experiments.

There are at least three different classes of phenomena where the dynamics can be characterized by the theoretical results presented in this Letter. Some of them are very much relevant to previous experimental efforts. The first class of phenomena are boundary or surface dynamics in a topological state. Around a typical topological bulk, surface fermions are gapless and protected by symmetries [17–19]. Many aspects of interaction dynamics on gapless surfaces can be related to quantum critical phenomena [20], as was discussed in Ref. [21]. For instance, surface transport of a three-dimensional (3D) topological superfluid or superconductor shall resemble those in a quantum critical regime in 2D. Consequently, surface thermal conductivity should scale in a way similar to that in quantum critical regimes in $d = 2$ (d being the spatial dimension) studied below, after a proper symmetry identification.

The second applicable class is the celebrated examples of superconductor–topological-insulator–superconductor (STIS) junctions with a π -phase shift between supercon-

ducting regions [6]. Just like surface states discussed above, STIS junctions host gapless Majorana fermions confined along one spatial direction. Thermal conductivity of a 1D channel in this case can also be directly related to dynamics near 1D quantum critical points.

The last class is related to quantum critical regimes where universality classes are defined by emergent gapless *real* fermions, which also turn out to be topological in nature. Generally, between quantum phases with same local ordering but different topologies, there shall always be topological quantum critical points (TQCPs). These TQCPs are not induced by usual spontaneous symmetry breaking, and are beyond the standard Landau paradigm of order-disorder phase transitions. Instead, they appear to signify a change of global topologies. A particularly interesting subset is the TQCPs in fermionic superfluids and superconductors [21–23]. One unique aspect of superconductors is that particle and hole excitations are indistinguishable due to the presence of the condensate of Cooper pairs. Thus, TQCPs in superconductors are naturally characterized by dynamics of Majorana fermions.

Below we will carry out our discussions in the context TQCPs although one shall keep in mind that their main practical applications are to gapless or nearly gapless Majorana fermions in superconductors or superfluids that are experimentally more accessible. In a few previous papers by the authors and collaborators [21–23], we have developed effective field theories of real fermions interacting with massive real scalar fields to describe TQCPs in fermionic superfluids and superconductors. These TQCPs separate topological and non-topological states that are both superfluids or superconducting. Topological phase transitions between these states happen only at zero temperature; at finite temperatures, states crossover into each other. In this Letter, we first investigate interacting gapless real fermions in this particular context

and focus on how discrete global symmetries such as a Z_2 time-reversal symmetry (TRS) affect thermodynamic and transport properties near TQCPs in superfluids and superconductors. We will discuss applications to other gapless systems afterwards.

The motivation to study the effect of global symmetries is at least two-fold. First, the classification of (weakly interacting) topological superfluids and superconductors depends on global symmetries such as TRS [24–27]. For example, in two dimensions superconductors with no global symmetry (i.e. *breaking TRS*) are classified by the integer group Z , while superconductors *with TRS* are classified by the Z_2 group. Thus, one should expect that TQCPs with different global symmetries to be assigned to quantum phase transitions between topological states and topologically trivial states. Second, at more conventional quantum critical points involving order-disorder transitions, global symmetries play a central role in determining their universality [20]. Therefore, it is also natural to investigate the roles of global symmetries at TQCPs beyond the standard Landau paradigm.

The key concept here is that it is global symmetries at TQCPs that define the degrees of freedom at low energies [23]. For example, if apart from the particle-hole symmetry no other symmetries are present, generically the low energy effective field theory should only consist of a minimum $n = 2$ or two-component real fermion fields in its fundamental representation. This case of no global symmetries can also be named as the case of Z_1 .

If there do exist discrete global symmetries, the effective field theory should consist of $n = 2N$ -component Majorana fermions with $N > 1$. In particular, if only a Z_2 global symmetry such as TRS is present, we have an $n = 2N = 4$ real-fermion field representation for TQCPs. The differences in $2N$, the degrees of freedom near TQCPs, dictate the structure of effective interactions, which in turn determines the universal behavior of thermodynamic and transport quantities in the quantum critical regime.

For strongly interacting TQCPs, the effect of global symmetries has been analyzed before. The presence of global symmetries does change the universality of these TQCPs as suggested in Ref. [23]. On the other hand, for weakly interacting TQCPs between gapped superfluid or superconducting phases, Z_2 global symmetries, such as TRS, are found not to change the universal scaling of *thermodynamic quantities* near TQCPs or the order of phase transitions [22] in high dimensions $d = 2, 3$. However, as to be elaborated in this Letter, the entropy density and scaling of dynamics such as thermal conductivity are distinct in quantum critical regimes with and without any global symmetries. Practically, they can be robust smoking guns for detecting underlying global symmetries and their impact on relevant degrees of freedom in emergent real fermion dynamics.

Before discussing details, we would like to emphasize

again that although the following scaling of thermal conductivity is obtained in the context of TQCPs, it can be applied to other gapless or nearly gapless Majorana systems that are experimentally accessible, such as surface Majorana states of topological superconductors and gapless states in 1D Majorana wire built of STIS junctions.

For concreteness, we use a Z_2 symmetry of TRS as an example to demonstrate the effect of global symmetries. We compare TQCPs with no symmetry (referred as time-reversal breaking or TRB for short) and those with only TRS (referred as time-reversal invariant or TRI). The generic low energy effective Hamiltonian for TQCPs between fully gapped superfluid or superconducting phases has the following emergent relativistic form

$$\mathcal{H} = \frac{1}{2}\psi^T \left[c_\psi \sum_{j=1}^d (-i\partial_j)\Gamma_j + \Gamma_0 m \right] \psi + \mathcal{H}_{\text{int}} \quad (1)$$

where

$$\mathcal{H}_{\text{int}} = \frac{1}{2} [\pi^2 + c_\phi^2 (\nabla\phi)^2 + M^2\phi^2] + g\psi^T \Gamma_0 \psi \phi, \quad (2)$$

ψ is a $n = 2$ two-component real field for Z_1 or TRB case, and a $n = 4$ four component real fermion field for Z_2 symmetric case or TRI case. ϕ is a massive real scalar field, π is the canonical conjugate field of ϕ , and d is the spatial dimension. Here, we focus on a generic model where Majorana fermions only couple to one single most relevant scalar field.

TRB topological superconductors only exist in 2D and are comprised of spinless fermions, with $\psi = (\chi_+, \chi_-)^T$ and

$$\Gamma_1 = \tau_z, \quad \Gamma_2 = \tau_x, \quad \Gamma_0 = \tau_y. \quad (3)$$

TRI topological superconductors comprised of spin-1/2 fermions exist in both 2D and 3D, with $\psi = (\chi_{+\uparrow}, \chi_{+\downarrow}, \chi_{-\uparrow}, \chi_{-\downarrow})^T$ and

$$\Gamma_1 = -\tau_z \sigma_z, \quad \Gamma_2 = \tau_x \sigma_0, \quad \Gamma_3 = \tau_z \sigma_x, \quad \Gamma_0 = \tau_y \sigma_0. \quad (4)$$

τ_α and σ_α ($\alpha = x, y, z$) are Pauli matrices in the (χ_+, χ_-) and spin subspaces, respectively, with σ_0 being the identity matrix.

The effective Hamiltonian is valid in the vicinity of the TQCP where real fermions are almost massless but ϕ field is always massive [22] unless further fine tuned so that the TQCP falls into a conformal fixed point. Generically, near TQCPs, we can have $m \ll \Lambda_0 \ll M$, with Λ_0 being the ultraviolet momentum cutoff of the effective theory.

Let us first focus on the weakly interacting case. A direct consequence of different degrees of freedom near TQCPs due to different symmetries is different amounts of thermal entropy in the quantum critical regime. The degrees of freedom near a TRI TQCP is twice that of a TQCP with no symmetries. Thus, thermal entropy in the quantum critical regime should also be twice for systems

with only TRS compare with those without any symmetries. Near a weakly interacting TQCP, interactions always flow to zero. Therefore, we can approximate the thermal entropy density S in the quantum critical regime using simple thermodynamic relations for noninteracting systems and find for $T \gg m$,

$$S \approx (2s+1)(d+1)\alpha_d c_\psi^{-d} T^d, \quad (5)$$

where s is the total spin, and $\alpha_d = (2\pi)^{-d} \Omega_{d-1} \int dx x^{d-1} \ln(1+e^{-x})$, with Ω_{d-1} the solid angle for a $(d-1)$ -sphere. Note that a TRI system has $s = 1/2$, while a TRB system has $s = 0$. Thus, although the entropy always scales as T^d regardless of global symmetries, the value of entropy density measured in units of $(T/c_\psi)^d$ is doubled when a Z_2 symmetry is present; so is the specific heat C_V that directly measures the entropy.

Another aspect of different symmetries is the scaling of transport properties such as thermal conductivity. For the weakly interacting case, since the scalar field ϕ is too massive to be excited, it is the elastic scattering between fermions that enters thermal conductivity. TRS plays an important role in determining the scaling of the scattering amplitude. In the following, we consider scattering between two-component Majorana fermions with given spin $(\chi_{+,s_i}, \chi_{-,s_i})^T$ (Fig.1).

The scattering amplitude has the following form

$$a(1, 2; 3, 4) \propto g^2 \left[\frac{\delta_{s_1, -s_2} \delta_{s_1, s_3} \delta_{s_2, s_4}}{(\epsilon_1 - \epsilon_3)^2 - c_\phi^2 (\mathbf{k}_1 - \mathbf{k}_3)^2 - M^2 + i\delta} + \frac{\delta_{s_1, s_2} \delta_{s_1, s_3} \delta_{s_2, s_4}}{(\epsilon_1 - \epsilon_3)^2 - c_\phi^2 (\mathbf{k}_1 - \mathbf{k}_3)^2 - M^2 + i\delta} - \frac{\delta_{s_1, s_2} \delta_{s_1, s_4} \delta_{s_2, s_3}}{(\epsilon_1 - \epsilon_4)^2 - c_\phi^2 (\mathbf{k}_1 - \mathbf{k}_4)^2 - M^2 + i\delta} \right], \quad (6)$$

where the index i denotes two-component Majorana fermions with energy ϵ_i , momentum \mathbf{k}_i , and spin s_i .

For the TRB case of spinless fermions, the first term in the summation vanishes identically. The second (direct) and third (exchange) terms cancel in the leading order $O(\frac{1}{M^2})$ resulting in a subleading term of $O(\frac{1}{M^4})$ in the limit $M \gg \Lambda_0$,

$$a(1, 2; 3, 4) \propto \frac{g^2}{M^4} \left[(\epsilon_1 - \epsilon_4)^2 - c_\phi^2 (\mathbf{k}_1 - \mathbf{k}_4)^2 - (\epsilon_1 - \epsilon_3)^2 + c_\phi^2 (\mathbf{k}_1 - \mathbf{k}_3)^2 \right]. \quad (7)$$

Thus, for the Z_1 case without any symmetry, a vanishes in the infrared limit when the frequency and momentum approach zero with a scaling dimension $D_s = 2$.

In contrast, for the TRI case of spin-1/2 fermions, the first term in the summation of $O(\frac{1}{M^2})$ is dominating in the same limit, and we have

$$a(1, 2; 3, 4) \propto \frac{g^2}{M^2} \delta_{s_1, -s_2} \delta_{s_3, -s_4} \delta_{s_1, s_3}. \quad (8)$$

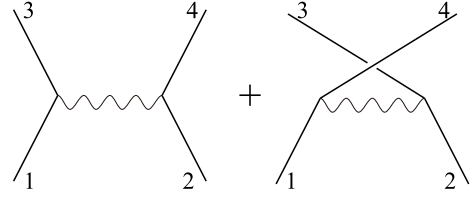


Figure 1. Effective fermion-fermion scattering in the massive scalar field limit. Solid lines represent two-component Majorana fermions with given spin, and wavy lines represent massive scalar fields.

a in the presence of a Z_2 global symmetry remains a constant in the infrared limit, in stark contrast to the Z_1 case without global symmetries.

The scattering amplitude between Majorana fermions sets the scattering rate between quasiparticles. This scattering rate can be obtained from Fermi's Golden rule [28]

$$\frac{1}{\tau_{sc}} = \frac{2\pi}{\hbar} \sum_{\substack{\mathbf{k}_2, \mathbf{k}_3, \mathbf{k}_4 \\ s_2, s_3, s_4}} \left\{ |\tilde{a}(1, 2; 3, 4)|^2 \delta(\epsilon_1 + \epsilon_2 - \epsilon_3 - \epsilon_4) (2\pi\hbar)^d \delta(\mathbf{k}_1 + \mathbf{k}_2 - \mathbf{k}_3 - \mathbf{k}_4) [f_2(1-f_3)(1-f_4) + (1-f_2)f_3f_4] \right\}, \quad (9)$$

where $f_i = 1/(e^{\epsilon_i} + 1)$ and $\epsilon_i = \sqrt{c_\psi^2 \mathbf{k}_i^2 + m^2}$ are the quasiparticle distribution function and energy, and $\tilde{a}(1, 2; 3, 4)$ is the scattering amplitude between quasiparticles with coherence factors further included [29, 30].

Accordingly, the scattering rate has the following scaling behaviors for low energy quasiparticles with $\epsilon_1 \sim O(T)$. For the TRB case, we have

$$\frac{1}{\tau_{sc}} \propto \frac{g^4}{M^8} T^{2d+3}. \quad (10)$$

In contrast, for the TRI case we have

$$\frac{1}{\tau_{sc}} \propto \frac{g^4}{M^4} T^{2d-1}. \quad (11)$$

As a result, thermal conductivity in the quantum critical regime should scale differently for systems with and without TRS. This can be seen by solving the Boltzmann equation

$$\partial_t f' + (\nabla_{\mathbf{k}} \epsilon_{\mathbf{k}}) \cdot (\nabla_{\mathbf{r}} f') - (\nabla_{\mathbf{r}} \epsilon_{\mathbf{k}}) \cdot (\nabla_{\mathbf{k}} f') = -\frac{f' - f}{\tau_{sc}}, \quad (12)$$

where $\nabla_{\mathbf{r}}$ and $\nabla_{\mathbf{k}}$ are gradients in spatial and momentum spaces, and f' and f are quasiparticle distribution functions away and at equilibrium. In the limit $m \rightarrow 0$, we have

$$\kappa = (2s+1)\tau_{sc} T^d c_\psi^{2-d} I_d, \quad (13)$$

where $I_d = \int \frac{d\Omega_{d-1}}{(2\pi)^d} \cos^2 \theta \int dx x^{d+1} \frac{e^x}{(1+e^x)^2}$.

Therefore, the thermal conductivity scales differently with temperature in the quantum critical regime for different symmetries. For the Z_1 or TRB case with no global symmetries, we have

$$\kappa \propto T^{-(d+3)}, \quad d = 1, 2, 3. \quad (14)$$

While for the Z_2 TRI case, it becomes

$$\kappa \propto T^{-(d-1)}, \quad d = 1, 2, 3. \quad (15)$$

This is one of the main results of this Letter. When applying these results, especially Eq.(15) to $d = 1$, we have assumed weak interactions do not result in a gap and fermions still remain gapless.

Without fine tuning, a topological superconductor typically is not gapless or quantum critical. However, practically the results above can be easily applied to other gapless Majorana systems. For example, the surface Majorana states of 3D topological superconductors are always gapless and can be viewed as quantum critical from a surface point of view [21]. Therefore, it might be more plausible to examine the role of global symmetries by studying thermal conductivity of surface states. There is a subtle difference between bulk and surface states. Since the degrees of freedom of surface states are half of those in the bulk, surface states with only one Z_2 global symmetry of TRS are described by two-component real fermions rather than four-component real fermions in the bulk, mapping the dynamics into the Z_1 case.

For instance, consider a 3D topological superconductor with a global Z_2 TRS described by Hamiltonian (1) and Γ matrices (4). The effective Hamiltonian on the xz -surface can be written as

$$\mathcal{H}_{\text{surf}} = \frac{1}{2} \tilde{\psi}^T c_{\psi} [\sigma_z (i\partial_x) - \sigma_x (i\partial_z)] \tilde{\psi} + \mathcal{H}_{\text{int}}, \quad (16)$$

where $\tilde{\psi} = (\chi_{+\uparrow}, \chi_{+\downarrow})^T$ is a two-component real fermion on the surface and \mathcal{H}_{int} is the same as Eq. (2). This effectively describes a two-dimensional weakly-interacting massless real system, which can be mapped into a 2D TQCP without any global symmetry, i.e. the Z_1 case. Thus, the surface transport properties of 3D topological superconductors should resemble the transport properties of a 2D TRB topological superconductor in the quantum critical regime. Consequently, the surface thermal conductivity should scale as Eq. (14) with $d = 2$. Since the surface states remain gapless as long as the bulk gap remains open, no fine-tuning is required to observe such dynamics.

As mentioned before, another interesting applicable system is a STIS junction with a π -phase shift between superconducting regions. Just like the surface states discussed above, STIS junctions respect TRS and has a global Z_2 symmetry; being on the edge, they also host minimum $n = 2$ or two-component gapless real fermions

confined to a 1D quantum wire. The thermal conductivity of such a 1D wire should scale as Eq. (14) with $d = 1$ for the Z_1 case or without global symmetries.

We would like to emphasize that different scalings of transport quantities and mass renormalization are unique to gapless Majorana fermions [31]. This difference arises from the fact that when no symmetry is present, TQCP dynamics are determined by minimum two-component Majorana fields. Two Majorana fermions cannot interact locally and there can be no four-fermion interactions without involving gradient operators. This is in stark contrast to complex fermions, where four-fermion local interactions (without gradient operators) typically dominate in the long wavelength limit.

Finally, let us briefly comment on strongly interacting cases. Details of thermal transport in this limit remain a challenging topic. Here we focus on transport properties dictated by strong coupling fixed points. The strong coupling limit corresponds to massless scalar fields or $M = 0$ limit. The one-loop renormalization group equation for g has the following form

$$\frac{d\tilde{g}^2}{d \ln(\Lambda/\Lambda_0)} = -\epsilon \tilde{g}^2 + c_d \tilde{g}^4, \quad (17)$$

where Λ and Λ_0 are the running and ultraviolet momentum cutoff, $\epsilon = 3 - d$, $\tilde{g}^2 = g^2/\Lambda^\epsilon$, and c_d is a numerical factor [23]. This suggests an *infrared stable strong coupling fixed point* at $M = 0$, $\tilde{g}_c^2 = c_d^{-1}\epsilon$ for dimensions $d = 3 - \epsilon < 3$. These strong coupling fixed points belong to the Gross-Neveu type and are represented by conformal field theories. The fixed point of the TRB case further exhibits supersymmetry in addition to the standard scale-conformal symmetry [23]. Nevertheless, in both TRB and TRI cases, dynamics are manifestly scale invariant, differing from the weakly coupling cases as the scalar field is now massless.

At finite T , the scalar fields shall develop a mass gap of order of $f(\tilde{g}_c^2)T$ where $f(\tilde{g}_c^2 = c_d^{-1}\epsilon)$ is a universal function that only depends on ϵ . In the standard ϵ -expansion, one obtains that $f(\epsilon) \propto \epsilon$ [30]. Following general considerations, the scattering rate has the following generic scaling form, for either TRI or TRB *strong coupling fixed points*, $\frac{\hbar}{\tau_{sc}} \propto \Lambda^z h(\tilde{g}(\Lambda), \frac{\Lambda^z}{T})$, where Λ is the ultraviolet scale of an effective field theory, $\tilde{g}(\Lambda)$ is the dimensionless coupling constant for a running scale Λ and $h(x, y)$ is a dimensionless function. $z = 1$ is the dynamic scaling exponent in our case.

The key idea here is that at strong coupling *fixed points*, $\tilde{g}(\Lambda) = \tilde{g}_c \sim \epsilon$ is independent of the running scale Λ . So by simply setting the running scale so that $\Lambda^z = T$, we find that the scattering rate $1/\tau_{sc}$ is naturally related to the Planckian time scale \hbar/T at fixed points, regardless of TRS. Indeed, we find that in $d = 3 - \epsilon$ (i.e. slightly below 3D) [30]

$$\frac{\hbar}{\tau_{sc}} = Th(\tilde{g}_c, 1) \propto \epsilon T. \quad (18)$$

Consequently, unlike in the weakly coupling limit where we have found distinctly different scaling properties, thermal conductivity at strong coupling fixed points shall always scale as, in both TRB and TRI cases,

$$\kappa \propto T^{d-1}. \quad (19)$$

So in this limit, scaling behaviors of thermal transport κ turn out to be the same with or without Z_2 global symmetries.

In conclusion, we have examined the effect of discrete global symmetries on interacting gapless Majorana fermions in superfluids and superconductors. We find that discrete global symmetries can set the values of entropy density and scaling properties of transport quantities such as thermal conductivity. Global symmetries determine degrees of freedom at low energies, which not only directly affect entropy but also put stringent constraints on effective fermion-fermion interactions. In this Letter, we have used TRS as an example to discuss these effects, but the results can be generalized to other global symmetries such as parity and to crystalline symmetries as well. We also note that scalings of thermal conductivity are applicable to many gapless Majorana systems that are quite accessible in experiments.

One of the applications of the results obtained in this Letter is to utilize them as an approach to detect Majorana fermions in the presence or absence of global symmetries as thermal transport properties are distinctly different. Generally, global symmetries such as TRS cannot be easily detected directly in experiments. The measurement on thermal conductivity can offer information about possible global symmetries present in interacting Majorana fermions.

F.Y. is supported by Chinese International Postdoctoral Exchange Fellowship Program (Talent-introduction Program) and Shuimu Tsinghua Scholar Program at Tsinghua University. F.Z. is supported by an NSERC (Canada) Discovery Grant under the contract RGPIN-2020-07070 and a grant from the University of British Columbia.

- [9] R. M. Lutchyn, J. D. Sau, and S. Das Sarma, *Phys. Rev. Lett.* **105**, 077001 (2010).
- [10] J. Alicea, *Phys. Rev. B* **81**, 125318 (2010).
- [11] S. B. Chung, H.-J. Zhang, X.-L. Qi, and S.-C. Zhang, *Phys. Rev. B* **84**, 060510(R) (2011).
- [12] A. Cook and M. Franz, *Phys. Rev. B* **84**, 201105(R) (2011).
- [13] S. Gangadharaiah, B. Braunecker, P. Simon, and D. Loss, *Phys. Rev. Lett.* **107**, 036801 (2011).
- [14] T.-P. Choy, J. M. Edge, A. R. Akhmerov, and C. W. J. Beenakker, *Phys. Rev. B* **84**, 195442 (2011).
- [15] A. Yu. Kitaev, *Ann. Phys.* **303** 2 (2003).
- [16] C. Nayak, S. H. Simon, A. Stern, M. Freedman, and S. Das Sarma, *Rev. Mod. Phys.* **80**, 1083 (2008).
- [17] M. Z. Hasan and C. L. Kane, *Rev. Mod. Phys.* **82**, 3045 (2010).
- [18] X.-L. Qi and S.-C. Zhang, *Rev. Mod. Phys.* **83**, 1057 (2011).
- [19] B. A. Bernevig and T. Hughes, *Topological insulators and topological superconductors* (Princeton University Press 2013).
- [20] S. Sachdev, *Quantum Phase Transitions 2nd Edition*, (Cambridge University Press, 2011).
- [21] F. Yang and F. Zhou, *Phys. Rev. B* **103**, 205126 (2021).
- [22] F. Yang, S.-J. Jiang, and F. Zhou, *Phys. Rev. B* **100**, 054508 (2019).
- [23] F. Zhou, *Phys. Rev. B* **105**, 014503 (2022).
- [24] A. P. Schnyder, S. Ryu, A. Furusaki, and A. W. W. Ludwig, *Phys. Rev. B* **78**, 195125 (2008).
- [25] A. Kitaev, *AIP Conference Proceedings* **1134**, 22 (2009).
- [26] X.-L. Qi, T. L. Hughes, and S.-C. Zhang, *Phys. Rev. B* **81**, 134508 (2010).
- [27] J. C. Y. Teo and C. L. Kane, *Phys. Rev. B* **82**, 115120 (2010).
- [28] P. Coleman, *Introduction to Many-body Physics*, (Cambridge University Press, 2015).
- [29] J. R. Schrieffer, *Theory of Superconductivity* (Addison-Wesley Publishing Company, 1964).
- [30] See Supplementary Material for details about coherence factors, mass renormalization of Majorana fermions, and scattering rate in strong coupling limit.
- [31] Global symmetries also affect the Majorana mass renormalization. For TRB systems with $s = 0$, in the large mass limit the Majorana mass renormalization is given by $\delta m \approx \frac{g^2 c_\psi \Lambda_0^3}{18\pi^2 M^4} \left(1 + \frac{2c_\psi^2}{c_\psi^2}\right) m$. However, for TRI systems with spin $s = 1/2$, the Majorana mass renormalization becomes $\delta m \approx (2s) \frac{g^2 \Lambda_0}{2\pi^2 M^2 c_\psi} m$. See Supplementary for detail. The expression for $\delta\mu$ below Eq. (30) in Ref. [22] is only valid for TRI cases.

-
- [1] J. Alicea, *Rep. Prog. Phys.* **75**, 076051 (2012)
- [2] C. W. J. Beenakker, *Annu. Rev. Condens. Matter Phys.* **4** 113 (2013).
- [3] S. R. Elliott and M. Franz, *Rev. Mod. Phys.* **87**, 137 (2015).
- [4] N. Read and D. Green, *Phys. Rev. B*, **61**, 10267 (2000).
- [5] A. Kitaev, *Phys.-Uspekhi* **44**, 131 (2001).
- [6] L. Fu and C. L. Kane, *Phys. Rev. Lett.* **100**, 096407 (2008).
- [7] X.-L. Qi, T. L. Hughes, and S.-C. Zhang, *Phys. Rev. B* **82**, 184516 (2010).
- [8] J. D. Sau, R. M. Lutchyn, S. Tewari, and S. Das Sarma, *Phys. Rev. Lett.* **104**, 040502 (2010).

Supplementary Material

Quasiparticle scattering amplitude

The scattering amplitude of quasiparticles $\tilde{a}(1, 2; 3, 4)$ differs from that of Majorana fermions $a(1, 2; 3, 4)$ due to the presence of coherence factors. For the TRB case, \tilde{a} is

$$\tilde{a}(1, 2; 3, 4) \propto \frac{g^2}{M^4} \left\{ [(\epsilon_1 - \epsilon_4)^2 - c_\phi^2(\mathbf{k}_1 - \mathbf{k}_4)^2] 2(u_{\mathbf{k}_1}^* u_{\mathbf{k}_4} - v_{\mathbf{k}_1} v_{\mathbf{k}_4}^*) 2(u_{\mathbf{k}_2}^* u_{\mathbf{k}_3} - v_{\mathbf{k}_2} v_{\mathbf{k}_3}^*) \right. \\ \left. - [(\epsilon_1 - \epsilon_3)^2 + c_\phi^2(\mathbf{k}_1 - \mathbf{k}_3)^2] 2(u_{\mathbf{k}_1}^* u_{\mathbf{k}_3} - v_{\mathbf{k}_1} v_{\mathbf{k}_3}^*) 2(u_{\mathbf{k}_2}^* u_{\mathbf{k}_4} - v_{\mathbf{k}_2} v_{\mathbf{k}_4}^*) \right\}. \quad (\text{S.1})$$

At TQCP, we have $u_{\mathbf{k}} = 1/\sqrt{2}$ and $v_{\mathbf{k}} = \Delta_{\mathbf{k}}/(\sqrt{2}|\Delta_{\mathbf{k}}|)$, where we have chosen $u_{\mathbf{k}}$ to be real and positive by convention. $\Delta_{\mathbf{k}}$ is the superconducting order parameter. For the TRB example considered in this Letter, we have $\Delta_{\mathbf{k}} = c_\psi(k_x + ik_y)$.

For the TRI case, we have

$$\tilde{a}(1, 2; 3, 4) \propto \frac{g^2}{M^2} 2(u_{\mathbf{k}_1}^\dagger u_{\mathbf{k}_3} - v_{\mathbf{k}_1} v_{\mathbf{k}_3}^\dagger)_{s_1 s_3} 2(u_{\mathbf{k}_2}^\dagger u_{\mathbf{k}_4} - v_{\mathbf{k}_2} v_{\mathbf{k}_4}^\dagger)_{s_2 s_4} \delta_{s_1, -s_2} \delta_{s_1, s_3} \delta_{s_2, s_4}. \quad (\text{S.2})$$

Here $u_{\mathbf{k}}, v_{\mathbf{k}}$ are 2×2 matrices. At the TQCP, we have $u_{\mathbf{k}\sigma\sigma'} = \delta_{\sigma\sigma'}/\sqrt{2}$, and $v_{\mathbf{k}\sigma\sigma'} = \Delta_{\mathbf{k}\sigma\sigma'}/\sqrt{2(\Delta_{\mathbf{k}}\Delta_{\mathbf{k}}^\dagger)_{\sigma\sigma}}$. For the TRI examples considered in this Letter, $\Delta_{\mathbf{k}} = c_\psi i\boldsymbol{\sigma} \cdot \mathbf{k}\sigma_y$.

Majorana mass renormalization in the weak coupling limit

Global symmetries affect the Majorana mass renormalization in the weak coupling limit, which is given by the diagrams in Fig. S.1. The two diagrams differ by a factor of $-(2s+1)$ as a result of the fermion loop in the second one. For TRB systems with $s=0$, the two diagrams exactly cancel each other in the order of $1/M^2$ in the large mass limit $M \gg \Lambda_0$. Thus, the Majorana mass renormalization is given by

$$\delta m^{(B)} \approx \frac{g^2 c_\psi \Lambda_0^3}{18\pi^2 M^4} \left(1 + \frac{2c_\phi^2}{c_\psi^2} \right) m. \quad (\text{S.3})$$

However, for TRI systems with spin $s=1/2$, these two diagrams no longer cancel in the order of $1/M^2$, and the Majorana mass renormalization becomes

$$\delta m^{(I)} \approx (2s) \frac{g^2 \Lambda_0}{2\pi^2 M^2 c_\psi} m. \quad (\text{S.4})$$



Figure S.1. One-loop diagram for the fermion propagator.

Strong coupling limit

We discuss the detailed structure of the imaginary part of self-energy near strong coupling fixed point. For simplicity, we focus on the case where $c_\phi = c_\psi = 1$. The scalar field acquires a finite mass at $T > 0$ and $d < 3$. Let $\epsilon = 3 - d$, we have

$$M^2 = (2s+1)g^2 T^{d-1} \int \frac{d^d x}{(2\pi)^d} \frac{1}{x(e^x + 1)}. \quad (\text{S.5})$$

As $g_c^2 \sim \epsilon T^{3-d}$, we have $M^2 \sim \epsilon T^2$.

The imaginary part of the on-shell retarded self-energy can be written as

$$\text{Im}\Sigma^R(\epsilon_{\mathbf{k}}, \mathbf{k}) = \text{Im}\Sigma_I^R(\epsilon_{\mathbf{k}}, \mathbf{k})I + \text{Im}\Sigma_j^R(\epsilon_{\mathbf{k}}, \mathbf{k})\Gamma_j, \quad (\text{S.6})$$

where I is the identity matrix, the repeated index j is summed over from 1 to d .

We have

$$\begin{aligned} \text{Im}\Sigma_0^R(\epsilon_{\mathbf{k}}, \mathbf{k}) = & -\pi g^2 \int \frac{d^d q}{(2\pi)^d} \frac{1}{4\xi_{\mathbf{q}}} \left\{ (1 - f_{\mathbf{k}-\mathbf{q}} + n_{\mathbf{q}}) [\delta(\epsilon_{\mathbf{k}} - \xi_{\mathbf{q}} - \epsilon_{\mathbf{k}-\mathbf{q}}) + \delta(\epsilon_{\mathbf{k}} + \xi_{\mathbf{q}} + \epsilon_{\mathbf{k}-\mathbf{q}})] \right. \\ & \left. + (f_{\mathbf{k}-\mathbf{q}} + n_{\mathbf{q}}) [\delta(\epsilon_{\mathbf{k}} - \xi_{\mathbf{q}} + \epsilon_{\mathbf{k}-\mathbf{q}}) + \delta(\epsilon_{\mathbf{k}} + \xi_{\mathbf{q}} - \epsilon_{\mathbf{k}-\mathbf{q}})] \right\}, \end{aligned} \quad (\text{S.7})$$

and

$$\begin{aligned} \text{Im}\Sigma_j^R(\epsilon_{\mathbf{k}}, \mathbf{k}) = & \pi g^2 \int \frac{d^d q}{(2\pi)^d} \frac{k_j - q_j}{4\xi_{\mathbf{q}}\epsilon_{\mathbf{k}-\mathbf{q}}} \left[(1 - f_{\mathbf{k}-\mathbf{q}} + n_{\mathbf{q}}) (\delta(\epsilon_{\mathbf{k}} - \xi_{\mathbf{q}} - \epsilon_{\mathbf{k}-\mathbf{q}}) - \delta(\epsilon_{\mathbf{k}} + \xi_{\mathbf{q}} + \epsilon_{\mathbf{k}-\mathbf{q}})) \right. \\ & \left. + (f_{\mathbf{k}-\mathbf{q}} + n_{\mathbf{q}}) (-\delta(\epsilon_{\mathbf{k}} - \xi_{\mathbf{q}} + \epsilon_{\mathbf{k}-\mathbf{q}}) + \delta(\epsilon_{\mathbf{k}} + \xi_{\mathbf{q}} - \epsilon_{\mathbf{k}-\mathbf{q}})) \right]. \end{aligned} \quad (\text{S.8})$$

Here $\epsilon_{\mathbf{k}-\mathbf{q}} = |\mathbf{k} - \mathbf{q}|$, $\xi_{\mathbf{q}} = \sqrt{q^2 + M^2}$, $f_{\mathbf{k}-\mathbf{q}} = 1/(e^{\epsilon_{\mathbf{k}-\mathbf{q}}} + 1)$, and $n_{\mathbf{q}} = 1/(e^{\xi_{\mathbf{q}}} - 1)$. For $M > 0$, only $\delta(\epsilon_{\mathbf{k}} - \xi_{\mathbf{q}} + \epsilon_{\mathbf{k}-\mathbf{q}})$ can be satisfied. This puts a constraint on the angle between \mathbf{k} and \mathbf{q} for each given $\xi_{\mathbf{q}}$.

The δ -function can be rewritten as

$$\delta(\epsilon_{\mathbf{k}} - \xi_{\mathbf{q}} + \epsilon_{\mathbf{k}-\mathbf{q}}) = \delta(\cos\theta - \cos\theta_0) \left(\frac{\sqrt{1 + M^2/q^2}}{k} - \frac{1}{q} \right) \Theta_1 \Theta_2 \Theta_3, \quad (\text{S.9})$$

where θ is the angle between \mathbf{k} and \mathbf{q} ,

$$\cos\theta_0 = \sqrt{1 + \frac{M^2}{q^2}} - \frac{M^2}{2kq}, \quad (\text{S.10})$$

$$\Theta_1 = \Theta(\sqrt{q^2 + M^2} - k), \quad (\text{S.11})$$

$$\Theta_2 = \Theta\left(q - k + \frac{M^2}{4k}\right), \quad (\text{S.12})$$

$$\Theta_3 = \Theta\left(k^2 - \frac{M^4}{8q^2 + 4M^2 + 8q\sqrt{q^2 + M^2}}\right), \quad (\text{S.13})$$

and $\Theta(\cdot)$ is the Heaviside step function.

Thus, we have

$$\text{Im}\Sigma^R(\epsilon_{\mathbf{k}}, \mathbf{k}) = -\pi g^2 \int \frac{d^d q}{(2\pi)^d} \left[(f_{\mathbf{k}-\mathbf{q}} + n_{\mathbf{q}}) \left(\frac{\sqrt{1 + M^2/q^2}}{k} - \frac{1}{q} \right) \delta(\cos\theta - \cos\theta_0) \Theta_1 \Theta_2 \Theta_3 \right] \left(\frac{1}{4\xi_{\mathbf{q}}} I + \frac{k_j - q_j}{4\xi_{\mathbf{q}}\epsilon_{\mathbf{k}-\mathbf{q}}} \Gamma_j \right), \quad (\text{S.14})$$

where the summation over index j is assumed. For $d = 3 - \epsilon$, we can first perform the angular integration, this restricts the direction of \mathbf{q} for each given \mathbf{k} . The step functions puts a constraint on the minimum value of q . Although $\text{Im}\Sigma^R(\epsilon_{\mathbf{k}}, \mathbf{k})$ is anisotropic, all its entries have the same scaling in T . For $\epsilon_{\mathbf{k}} \approx M/2$, the step functions can be satisfied for $q_{\min} \rightarrow 0$. In this case, each entry of $\text{Im}\Sigma^R(\epsilon_{\mathbf{k}}, \mathbf{k})$ is proportional to

$$g^2 T^{d-2} \ln \epsilon \propto T \epsilon \ln \epsilon, \quad \epsilon_{\mathbf{k}} \approx \frac{M}{2}. \quad (\text{S.15})$$

For $\epsilon_{\mathbf{k}} \gg M/2$, the step functions require that $q_{\min} \gtrsim k \gg M$. For $\epsilon_{\mathbf{k}} \ll M/2$, the step functions require $q_{\min} \gg M^2/k \gg M$. In both cases, each entry of $\text{Im}\Sigma^R(\epsilon_{\mathbf{k}}, \mathbf{k})$ is proportional to

$$g^2 T^{d-2} \propto \epsilon T, \quad \epsilon_{\mathbf{k}} \ll \frac{M}{2} \quad \text{or} \quad \epsilon_{\mathbf{k}} \gg \frac{M}{2}. \quad (\text{S.16})$$

For the typical case, the fermion energy $\epsilon_{\mathbf{k}}$ is of the order $O(T)$, which is much larger than $M/2 \sim O(\epsilon T)$. Only a negligibly small fraction (much smaller than ϵ) of fermions have energy $\epsilon_{\mathbf{k}} \approx M/2$. The scattering rate between quasiparticles is determined by $\text{Im}\Sigma^R(\epsilon_{\mathbf{k}}, \mathbf{k})$. The coherence factors only contribute coefficients of order one and do not change the scaling. Thus, the scattering rate has the following scaling

$$\frac{1}{\tau_{sc}} \propto \epsilon T. \quad (\text{S.17})$$